ISSN 0965-5425, Computational Mathematics and Mathematical Physics, 2014, Vol. 54, No. 3, pp. 491–504. © Pleiades Publishing, Ltd., 2014.
Original Russian Text © A.M. Gumerov, E.G. Ekomasov, F.K. Zakir'yanov, R.V. Kudryavtsev, 2014, published in Zhurnal Vychislitel'noi Matematiki i Matematicheskoi Fiziki, 2014, Vol. 54, No. 3, pp. 481–495.

Structure and Properties of Four-Kink Multisolitons of the Sine-Gordon Equation

A. M. Gumerov, E. G. Ekomasov, F. K. Zakir'yanov, and R. V. Kudryavtsev

Bashkir State University, ul. Zaki Validi 32, Ufa, 450076 Bashkortostan, Russia

e-mail: bgu@bk.ru, ekomasoveg@gmail.com, farni@rambler.ru

Received July 26, 2013; in final form, September 24, 2013

Abstract—The dynamics of nonlinear waves of the sine-Gordon equation with a spatially modulated periodic potential are studied using analytical and numerical methods. The structure and properties of four-kink multisolitons excited on two identical attracting impurities are determined. For small-amplitude oscillations, an analytical spectrum of the oscillations is obtained, which is in qualitatively agreement with the numerical results.

DOI: 10.1134/S0965542514030075

Keywords: sine-Gordon equation, four-kink multisolitons, structure and properties of solitons, numerical-analytical study.

1. INTRODUCTION

The sine-Gordon equation (SGE), whose solutions have the form of nonlinear solitary waves (solitons), is extensively used in various fields of science, for example, for describing wave processes in rocks, DNA dynamics in molecular biology, the dynamics of domain walls in magnets, dislocations in crystals, and fluxons in Josephson junctions [1–6]. In many cases, the behavior of solitons can be described within the framework of the point particle model; then their temporal evolution is governed by ordinary differential equations [7]. If perturbations are taken into account, the structure of solitons changes greatly and the solitons themselves have to be described as deformable particles [3]. Moreover, a characteristic feature of solitons is the excitation of internal degrees of freedom, which can play a determining role in some physical processes. The internal modes include translational and fluctuation ones, the latter associated with long-lived oscillations of the soliton width [8].

An issue of much interest is the influence exerted by perturbations of various shapes on the excitation of internal soliton modes of the SGE. The effect of small perturbations on SGE solutions can be studied using the well-developed perturbation theory for solitons [3, 7, 9, 10], while the effect of large perturbations can generally be investigated only with the help of numerical methods [11–14]. Since the SGE describes many phenomena in various areas of physics and engineering, a natural problem is to solve this equation in the presence of local inhomogeneities (see, e.g., [3]). For example, numerous works have studied the influence of a coordinate- and time-dependent external force described by a deltalike, steplike, hyperbolic, or harmonic function [15–18].

Another interesting case is a spatial modulation (inhomogeneity) of the periodic potential, or the presence of an impurity in the system [3, 7]. The interaction of SGE kinks with impurities in the one-dimensional case has long been discussed in the literature [3, 9, 11, 19]. For example, the classical particle model for the kink–impurity interaction is applicable in the case when the impurity does not admit the existence of an impurity mode, i.e., a localized oscillatory state on the impurity. The importance of impurity modes in kink–impurity interactions was shown in [14, 17, 20–25]. In recent years, the kink–impurity interaction has been investigated in the two-dimensional case [26–28]. Much attention has been given to multisoliton solutions of the SGE [21, 29].

Consider the modified SGE (see [3, 7, 9])

$$\frac{\partial^2\theta}{\partial t^2} - \frac{\partial^2\theta}{\partial x^2} + \frac{K(x)}{2}\sin 2\theta = 0, \tag{1}$$

where $K(x)$ is a function characterizing the spatial modulation of the periodic potential (or "impurity"). This problem is of interest in many physical applications, for example, for moving domain walls in ferromagnets with defects, where $K(x)$ can change its sign [4].

In the case $K(x) = 1$, Eq. (1) becomes the well-known SGE and has a solution in the form of a topological soliton (or kink)

$$\theta(x, t) = 2\arctan(\exp[\Delta(\vartheta_0)(x - \vartheta_0 t)]), \tag{2}$$

where $\Delta(\vartheta_0) = 1/\sqrt{1 - \vartheta^2}$ and ϑ_0 is a continuous parameter ($0 < \vartheta_0 < 1$) determining the velocity of the kink. Equation (1) also has a spatially localized solution, namely, a quiescent breather

$$\theta_{im}(x, t, \omega) = 2\arctan\left(\frac{\sqrt{1 - \omega^2}\sin(\omega t)}{\omega\cosh(\sqrt{1 - \omega^2}(x - x_0))}\right),$$

where ω is the breather frequency and x_0 is the coordinate of its center.

By applying analytical and numerical methods, the dynamics of SGE solitons have been studied in detail in the case of a "point impurity," i.e., $K(x) = 1 - \varepsilon\delta(x)$, where $\delta(x)$ is the Dirac delta function and $0 < \varepsilon < 1$ (see [3, 7]). It was shown that, in the undeformable kink approximation, the impurity is equivalent to an effective potential. For example, for $\varepsilon > 0$, the impurity acts on a kink as an attracting potential; moreover, SGE kinks can be localized on the impurity and radiate [3]. In the case of a deformable kink, in addition to the oscillatory motion of the kink in the potential generated by the impurity, kink deformations of resonance nature (for example, a great change in the kink shape) occur [3]. The possibility of exciting an impurity mode as a result of kink scattering was also taken into account, which leads to a considerable change in the kink dynamics [14, 17, 21]. Note an interesting effect such as the reflection of a kink by an attracting impurity due to the resonance energy exchange between the translational mode of the kink and the impurity mode. The case of several delta-shaped point impurities, which are of interest in some physical applications [30, 31], and even the case of a spatially modulated harmonic potential [32] were considered. Analytical and numerical methods [9, 11, 33, 34] were used to investigate the dynamics of SGE kinks for steplike $K(x)$. In the case of a spatially extended impurity, for example, of the form

$$K(x) = \begin{cases} 1, & x < 0, \quad x > W, \\ 1 - \Delta K, & 0 \le x \le W, \end{cases} \tag{3}$$

where W is the width of the domain where the periodic potential is spatially modulated, the kink–impurity interaction was studied in both undeformable and deformable kink models [19, 22, 35]. The time dependences of the velocity and structure of a kink, soliton, and breather were found, and the minimum velocity required for a kink to escape from a potential well was determined.

Numerical methods were used in [22] to take into account the influence exerted on the dynamics of kinks by the nonlinear wave excited on the impurity. Specifically, as for a point impurity, the possibility of the resonance interaction between the kink and the excited impurity mode was shown numerically and analytically in [22]; moreover, the problem was solved without exactly analyzing the change in the kink structure caused by its interaction with the impurity. The structure and properties of localized nonlinear waves excited on an impurity were analyzed numerically in [23]. The case of an isotopic impurity [14] and a nontrivial metric of time [20, 36] were considered within the framework of the sine-Gordon model.

In the case of two identical impurities [37, 38], strong collective effects in the system were revealed, which can be used in kink pinning by the impurity to excite multisolitons of the SGE, for example, tritons and wobblers [38]. Additionally, it was shown that there can occur another interesting effect, namely, quasi-tunneling, in which case a kink passing through a double impurity needs less kinetic energy than that for passing a single impurity of the same sizes. However, the excitation, structure, and characteristics of SGE multisolitons in the case of several extended impurities have not been completely investigated. This paper deals with the dynamics of kinks of the one-dimensional sine-Gordon model with two identical spatially extended impurities of form (3) with the possibility of exciting localized large-amplitude nonlinear waves of the multisoliton type.

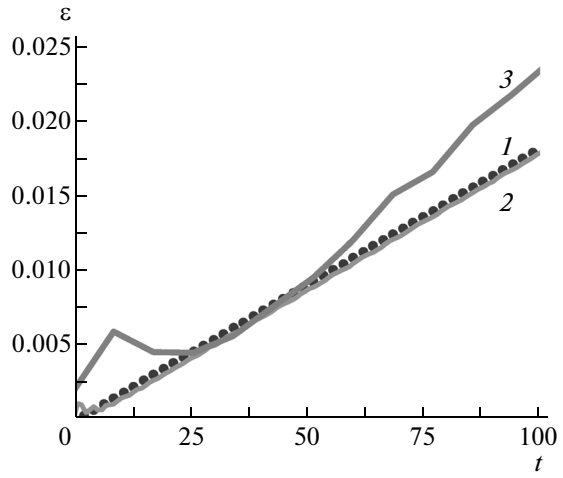

Fig. 1. Maximum normalized error ε accumulated by the numerical scheme in the course of a numerical experiment of typical duration as a function of time t for $N_x = (1)\ 10^5$, $(2)\ 10^4$, and $(3)\ 10^3$.

2. NUMERICAL RESULTS

The spatial modulation of a periodic potential is modeled as (see [38])

$$K(x) = \begin{cases} 1, & x < 0, \quad W < x < W + d, \quad x > 2W + d, \\ 1 - \Delta K, & 0 \le x \le W, \quad W + d \le x \le W + d, \end{cases} \tag{4}$$

i.e., in the form of two identical impurities separated by a distance d. Obviously, for a moving kink, an impurity is a potential well for $\Delta K > 0$ and a potential barrier for $\Delta K < 0$.

For the considered large values of ΔK, in the general case, we have to use numerical methods. Equation (1) is solved numerically by applying an explicit five-point finite-difference method [23, 37–39], which produces a grid function U_h whose values are approximately equal to the exact solution $U = 2\theta$ at grid points. In the framework of this method, the solution of Eq. (1) is reduced to computing the sought function at given grid nodes with the help of the recurrences

$$U_i^{n+1} = C_2(U_{i-1}^n + U_{i+1}^n) + C_3 U_i^n + C_4 U_i^{n-1} - K^*(x)\sin U_i^n, \tag{5}$$

where

$$K^*(x) = C_1 K(x), \quad C_1 = \Delta t^2, \quad C_2 = \frac{C_1}{\Delta x^2},$$
$$C_3 = C_1\left(\frac{2}{\Delta t^2} - \frac{2}{\Delta x^2}\right), \quad C_4 = -\frac{C_1}{\Delta t^2}. \tag{6}$$

Here, Δx is the spatial mesh size and Δt is the time step. Introducing the function $K^*(x)$, we can compute it prior to the simulation, thus eliminating one multiplication operation at every step. Numerical scheme (5), (6) is stable if $(\Delta t/\Delta x)^2 < 1$. This method was one of the first used to solve the SGE numerically [40]. A kink of form (2) moving at the constant velocity ϑ_0 was specified as an initial condition, and the boundary conditions were $\theta(-\infty, t) = 0$, $\theta(+\infty, t) = \pi$, and $\theta'(\pm\infty, t) = 0$.

The typical implementations of the numerical solution to Eq. (1) used in [23, 28, 35] make it possible to calculate the structure and dynamics of kinks with accuracy sufficient for observing the pinning of a kink by an impurity, its passage through an impurity, and the structure and properties of excited nonlinear waves. However, higher numerical accuracy is required for the study of possible resonance effects. For this reason, the function $\theta(x, t)$ was approximated using $N_x = 10^4$ points.

In connection with the increased requirements on the accuracy of the computations, we needed a procedure for monitoring the error of the results. The error accumulated in the course of the numerical experiment was estimated using the exact solution of Eq. (1) in the case $K(x) = 1$, i.e., kink (2) moving at a constant velocity. The numerical and analytical solutions are compared in Fig. 1. The error presented was

computed as follows: the maximum deviation of the numerical solution from the analytical one at a given time was normalized by the characteristic quantity π:

$$\varepsilon = \frac{1}{\pi}\max|\theta(x, t) - \theta^*(x, t)|,$$

where $\theta(x, t)$ is the numerical solution of Eq. (1) and $\theta^*(x, t)$ is analytical solution (2). It can be seen that even a slight improvement in the numerical accuracy requires that the number of approximation points be increased by an order of magnitude. Based on these results, $N_x = 10^4$ was found optimal and was used in the computations. Note that the largest influence one the accuracy of the computed dynamic characteristics of the simulated system (for example, on the frequency of the kink or breather center) was exerted not by the absolute value of the global error but rather by the amplitude of its "oscillation" (curves *1* and *2* in Fig. 1 are the most smooth).

Scheme (5), (6) was numerically implemented in Delphi [39]. Additionally, the algorithm was optimized to reduce the CPU time. Specifically, by using the specific properties of the problem and reducing the numerical accuracy and the range of the argument, the computation of the sine function was accelerated by more than eight times with the help of the polynomial approximation

$$\sin x \approx -4B(x)[1 + B^2(x)[A_3 + B^2(x)[A_5 + B^2(x)[A_7 + B^2(x)[A_9 + B^2(x)A_{11}]]]]], \quad (7)$$

where

$$B(x) = 0.25x + \pi/4, \quad A_7 = -0.79794217405921,$$
$$A_3 = -2.66592780638819, \quad A_9 = 0.16264977471553,$$
$$A_5 = 2.12775693434532, \quad A_{11} = -0.01573479830529.$$

With the use of approximate formula (7), the sine on the interval $[-2, 8]$ can be computed to 10^{-4} accuracy. The condition for finding the argument of the sine in this interval is ensured by monitoring the residual and the total energy of the system.

To optimize memory access operations, we used the built-in assembler of the Delphi compiler. As a result, rejecting the high-level programming language, we overcame many of its restrictions and produced a much more optimal code than that generated by the compiler. Tests showed that the overall acceleration of the computations due to the optimization performed was roughly five times as compared with the conventional implementation.

In the numerical experiments, a kink passed through impurities and its structure and basic dynamical characteristics were computed at each time. The possible variants of kink dynamics were as follows: the kink was pinned by the first or second impurity, the kink oscillated between them for a long time, and the kink was reflected in the opposite direction [38, 41]. In what follows, the case of the kink passing through both impurities is examined in more detail. In this case, the impurities give rise to oscillating localized large-amplitude nonlinear waves of the breather type (see Fig. 2c [23]), which have a large effect on the scattering of the kink. They are coupled four-kink multisoliton states, which are referred to hereafter as *quadrons*. A quadron can be treated as a multisoliton consisting of coupled two-kink breather states localized in each of these impurities. These states are referred to as *impurity modes*. Note that impurity modes are accompanied by radiating small-amplitude waves.

The numerical results for the general case showed that the character of the arising state of the system can be affected by varying two parameters: the initial kink velocity ϑ_0 and the distance d between the impurities. In-phase and antiphase oscillations, beats, and two interacting waves merging into one are observed in Fig. 2. The type of coupling between the excited localized nonlinear waves varies with d. Since impurity modes are excited not simultaneously but rather at time intervals Δt_0, we can assume that ϑ_0 also influences the initial phase difference of their oscillations.

It should be noted that, because of the interaction between the impurity modes, the oscillation amplitude is a function of time (periodic exchange of oscillation energy between the impurity modes, see Fig. 2). The case of beats (see Fig. 2c) is the most typical oscillation regime, while in-phase (Fig. 2d) and antiphase (Fig. 2b) oscillations are observed only in special cases. (In these cases, the frequency and amplitude of the breather are nearly independent of time and determined basically by ΔK and W, and the amplitude additionally depends on the initial kink velocity [23, 28].) Thus, the behavior of the system in the case of coupled impurity modes can be widely different from that occurring in the case of a single impurity.

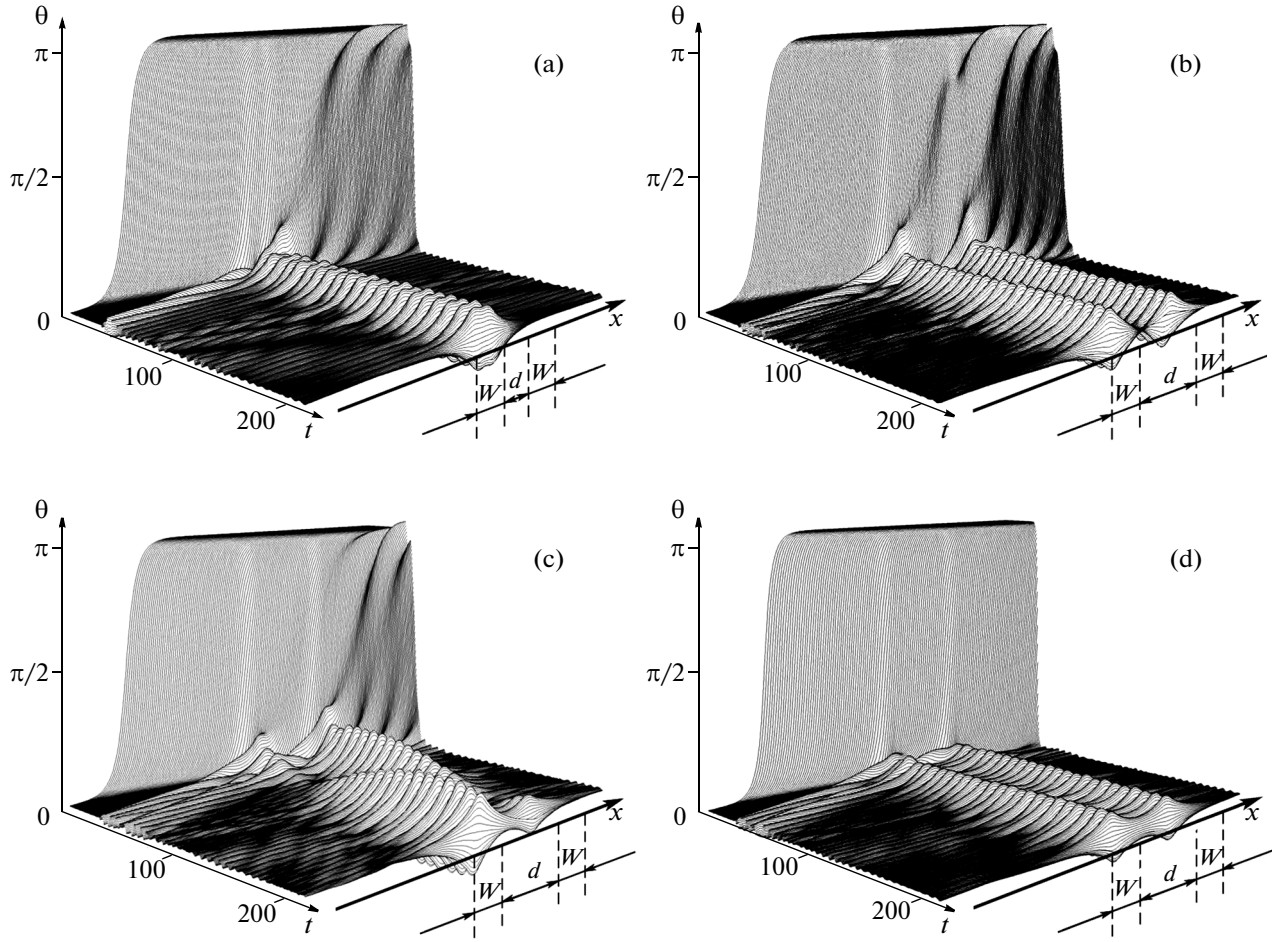

Fig. 2. Excitation and evolution of localized impurity modes on impurity (4) caused by a kink (with the initial velocity ϑ_0) passing through this impurity at $\Delta K = 1.2$ and $W = 1$ for (a) $d = 0.75$, $\vartheta_0 = 0.6$; (b) $d = 5$, $\vartheta_0 = 0.536$; (c) $d = 5$, $\vartheta_0 = 0.64$; and (d) $d = 5$, $\vartheta_0 = 0.782$.

2.1. The Case of Widely Spaced Impurities

Consider in more detail the case where the excited impurity modes are separated by a long distance (for example, $\Delta K = 1.2$ and $d > 4$). Let us find the time dependence of $R(t) = |\max(A) - \min(A)|$, where $A = A(\theta(x^*, t))$ is the instantaneous amplitude of an impurity mode (see Fig. 3). This quantity is convenient for measurement and automatic software analysis [39]. In fact, the energy "transfer" between the impurity modes is higher for larger values of R, but this is true only under the assumption that their frequency does not change greatly and the variation in the oscillation energy of each impurity mode is determined primarily by variations in its amplitude. Figure 4 shows R as a function of the initial kink velocity ϑ_0 for $d = 4$ and $d = 5$.

Let us examine in more detail the behavior of the system with $\Delta K = 1.2$ and $d = 5$ at three "singular" points $\vartheta_0 = 0.536, 0.64, 0.782$, which correspond to the extrema in curve *2* in Fig. 4a. The first and third points ($\vartheta_0 = 0.536, 0.782$) correspond to the minimum variation in the amplitude of the impurity modes, while the second point ($\vartheta_0 = 0.64$), to the maximum variation in this amplitude. Antiphase oscillations are observed at the first point, $\vartheta_0 = 0.536$ (see Fig. 5a). The amplitude (and the frequency $\omega_{im} = 0.8663$) are nearly independent of time. At the second point, $\vartheta_0 = 0.64$ (see Fig. 5b), the oscillation energy is transferred nearly completely from one impurity mode to the other (and back) over time. The arising oscillation regime is similar to beats exhibited by harmonic oscillators [42]. At the third point, $\vartheta_0 = 0.782$ (see Fig. 5c), as in the first case, the amplitude is nearly constant ($\omega_{im} = 0.8376$) but the oscillations are in phase.

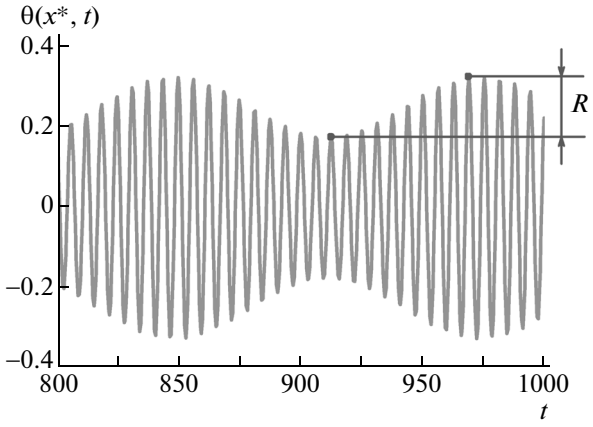

Fig. 3. Time dependence of $\theta(x^*)$, where x^* is the coordinate of the center of one of the impurities (3) and the definition of R (the amplitude of the envelope of impurity mode oscillations).

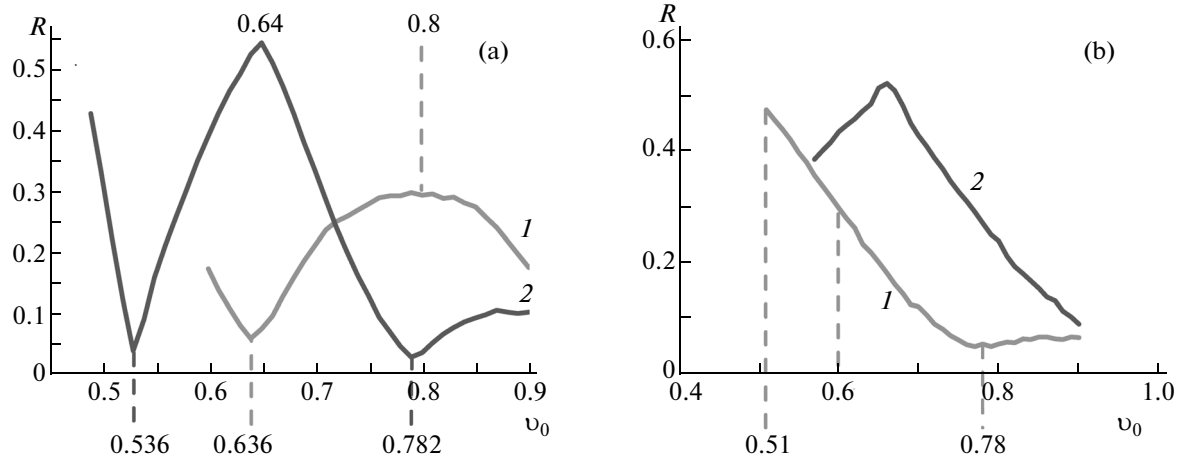

Fig. 4. The impurity mode envelope amplitude R as a function of the initial kink velocity ϑ_0 at $W = 1$ and $\Delta K = 1.2$: (a) (*1*) $d = 4$ and (*2*) $d = 5$, and (b) (*1*) $d = 2$ and (*2*) $d = 3$.

The Fourier spectral analysis of the impurity modes revealed two frequency components that are most pronounced in the beat regime (Fig. 5b) and are independent of ϑ_0 (i.e., of the initial phase difference between the impurity modes). Note that the Fourier spectrum contains only the first (lower) frequency component in the case of in-phase oscillations (Fig. 5c) and only the second (higher) frequency component in the case of antiphase oscillations (Fig. 5a). Thus, the quadron oscillations can be treated as the superposition of oscillations at two frequencies. Moreover, we can assume that these frequencies are associated with different states of the system: the lower frequency corresponds to in-phase oscillations, while the higher frequency, to antiphase oscillations.

Note that, in the case of single impurity (3) (see [38]), a single frequency was revealed for each pair of ΔK and W. For comparison purposes, Fig. 5 (curve *2*) presents the frequency spectrum of a single impurity. All the simulation parameters are the same. The only difference is that the double impurity is replaced by a single one. It can be seen that the frequency of the single impurity mode lies between the frequency components of the quadron.

Below, we determine the condition for exciting oscillation regimes with a certain phase difference: $(0, \pi/2, \pi)$. Let Δt_0 denote the difference between the excitation times of impurity modes on the first and second impurities. By the excitation time of an impurity mode, we mean the time when the kink intersects the center of the corresponding impurity. Assume, for simplicity, that the initial phase difference between the impurity modes is linearly proportional to Δt_0. The ratio $\Delta t_0 / \overline{T}_{im}$ shows how many periods of the first

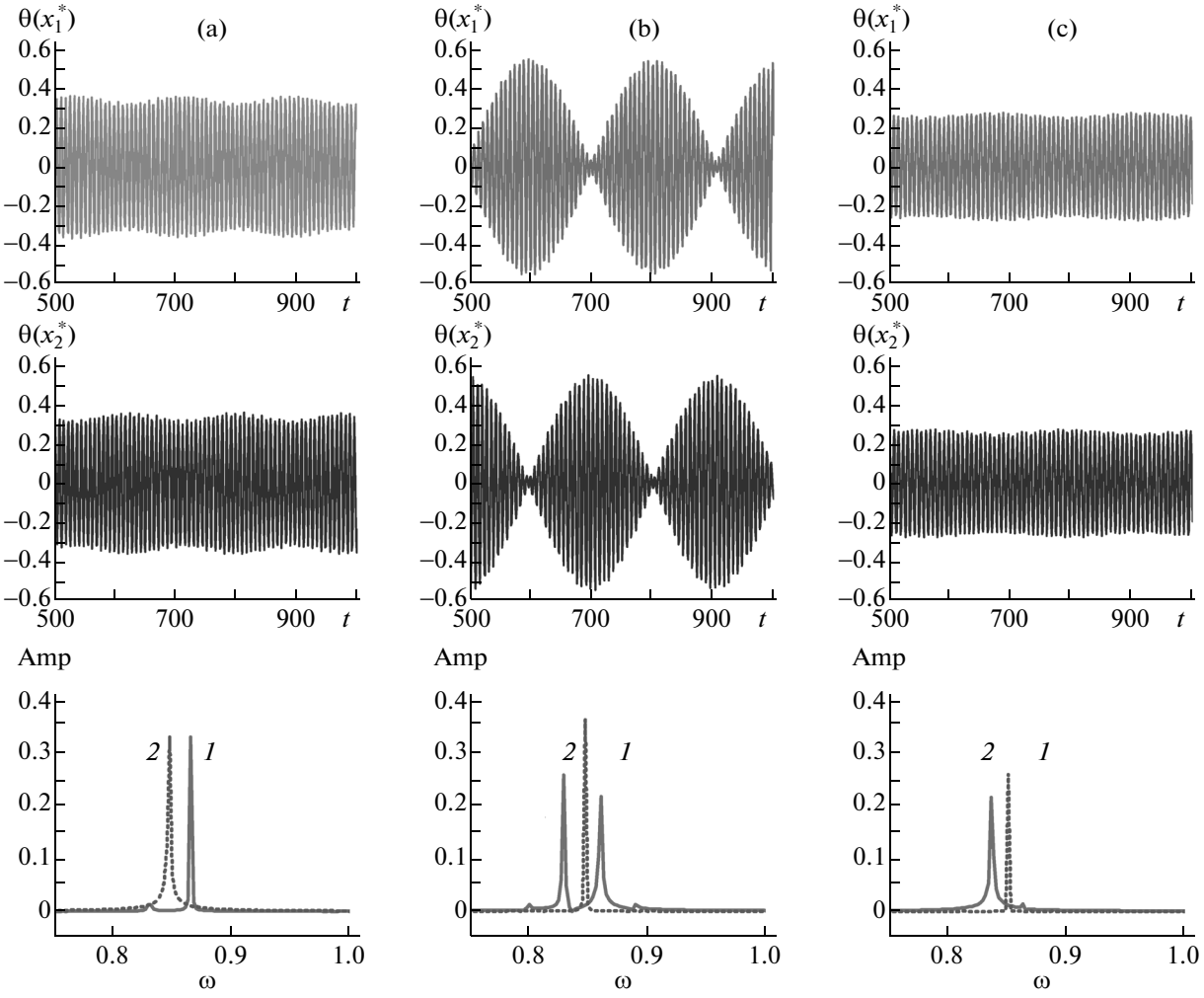

Fig. 5. Dependence of $\theta(x_i^*)$ on time t, where x_1^* and x_2^* are the coordinates of the centers of the first and second impurities, respectively. Amp(ω) is the Fourier spectrum of $\theta(x_1^*)$ (curve *1*) and the spectrum for the case of single impurity (3) at the same parameters W, ΔK, and ϑ_0 (curve *2*). The parameters are $W = 1$, $\Delta K = 1.2$, $d = 5$, and (a) $\vartheta_0 = 0.536$, (b) $\vartheta_0 = 0.64$, and (c) $\vartheta_0 = 0.782$.

impurity mode pass until the second impurity mode is excited. Of course, this value is approximate, since the first mode is assumed to oscillate at the constant averaged frequency $\overline{\omega}_{im}$ from the beginning of the excitation. Then the in-phase oscillation condition (an integer number of periods of the first impurity mode) and the antiphase oscillation condition (an odd number of half-periods of the same impurity mode) can be written as

$$\begin{aligned} \Delta t_0 &= n\overline{T}_{im}, \\ \Delta t_0 &= (2n+1)/2\overline{T}_{im}, \end{aligned} \tag{8}$$

where n is an integer and $\overline{T}_{im} = 2\pi/\overline{\omega}_{im}$. Maximal beats are observed in the "middle" between these states. Figure 6 shows Δt_0 vs. the initial kink velocity ϑ_0. For convenience, the points in these plots corresponding to the "extrema" in Fig. 4 (i.e., to the oscillation regimes with a certain phase difference: 0, π/2, or π) are given in the table together with the points computed using formulas (8).

It can be seen that, for $d = 5$, the points with phase differences 0, π/2, π agree well with formulas (8). For $d = 4$, the agreement is somewhat worse, which can be explained by the stronger interaction and energy transfer between the impurity modes.

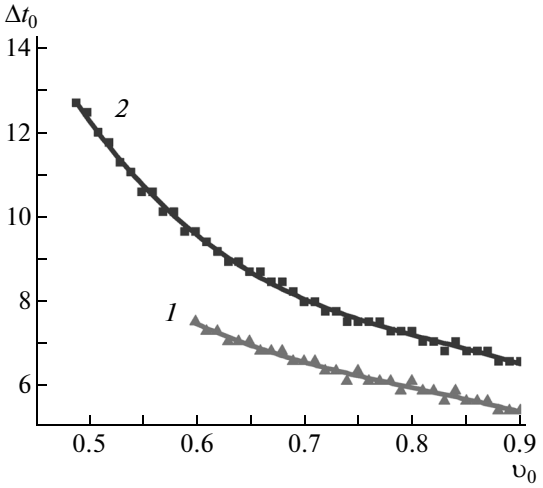

Fig. 6. Difference Δt_0 between the excitation times for the impurity modes excited by the first and second impurities as a function of the initial kink velocity ϑ_0. The labels show measured values, while the solid curves depict a cubic polynomial approximation. The parameters are $W = 1$, $\Delta K = 1.2$, and (*1*) $d = 4$ and (*2*) $d = 5$.

2.2. The Case of Closely Spaced Impurities

Now consider the case when excited impurity modes are separated by a short distance (for example, $\Delta K = 1.2$ and $d < 4$). More specifically, consider the cases $d = 2$ and $d = 3$. The general character of the dependence of R on ϑ_0 (see Fig. 4b) differs from the case of long distances between the impurities (Fig. 4a). By analogy with the case examined earlier, the oscillation regimes of the curve $d = 2$ are analyzed in more detail at three points: $\vartheta_0 = 0.51$, $\vartheta_0 = 0.6$, and $\vartheta_0 = 0.78$. At the first point, the amplitude of the impurity modes undergoes maximum variations with time (see Fig. 7a). The amplitude of the impurity modes at the third point nearly does not vary with time (Fig. 7c). The second point (Fig. 7b) is intermediate between these states. At the first point, $\vartheta_0 = 0.51$, the oscillation regime (Fig. 7a) is similar to previously considered ones where the energy of the impurity modes nearly completely passes from one to the other due to amplitude variations. At the second point, $\vartheta_0 = 0.6$ (Fig. 7b), the oscillation energy is transferred in a similar manner with the only difference being that the amplitude does not decrease to zero. At the third point, $\vartheta_0 = 0.78$, the amplitude of the impurity modes remains nearly constant and they oscillate in antiphase.

It should be noted that, for small d (in contrast to the above-considered case of large d), an arbitrary initial phase difference between the impurity modes cannot be obtained by varying ϑ_0. As a result, for example, in-phase oscillations of the impurity modes sometimes fail to be excited in the considered cases.

As the parameter d decreases further, a situation is observed when, for any initial ϑ_0, the phase difference between the impurity modes is reduced to zero and, after a certain time interval, they begin to oscillate in phase. Antisymmetric oscillations become unstable, and this oscillation regime fails to be excited. This is explained by the fact that, as $d \longrightarrow 0$, the binding energy considerably exceeds the oscillation energy of the impurity modes, which makes them oscillate in phase [42].

As was noted above, both frequency components in the frequency spectrum of the quadron (except for the special cases of in-phase and antiphase oscillations) are independent of ϑ_0. A further study has shown that similar behavior is exhibited for other values of d. In Fig. 8 curves *1* and *2* (triangle and squares, respectively) depict both frequencies as functions of d. Note that curve *2* is bounded away from zero, since only in-phase oscillations are stable for small d.

Oscillation regimes of impurity modes depending on the initial kink velocity

d	ϑ_0	Type	$\overline{\omega}_{\text{im}}$	$\overline{T}_{\text{im}}$	Δt_0	$\Delta t_0/\overline{T}_{\text{im}}$	n
5	0.536	Antiphase oscillations	0.8663	7.2529	11.19	1.5428	1
5	0.64	Beats	0.8450	7.4357	8.81	1.1848	–
5	0.782	In-phase oscillations	0.8376	7.5014	7.318	0.9755	1
4	0.636	In-phase oscillations	0.8232	7.6326	7.09	0.9289	1
4	0.8	Beats	0.8463	7.4243	5.95	0.8014	–

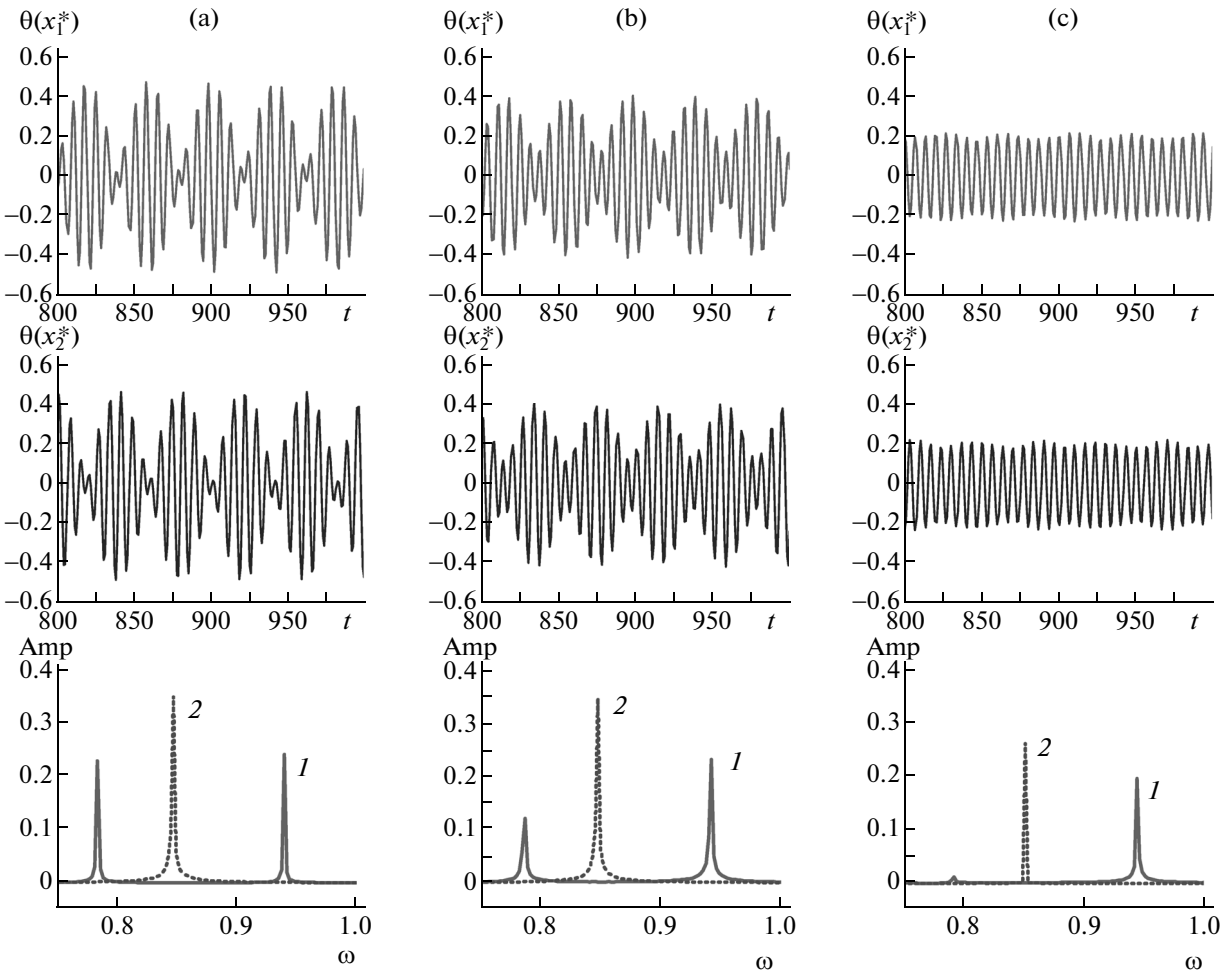

Fig. 7. Dependence of $\theta(x_i^*)$ on time t, where x_1^* and x_2^* are the coordinates of the centers of the first and second impurities, respectively. Amp(ω) is the Fourier spectrum of $\theta(x_1^*)$ (curve *1*) and the spectrum for the case of single impurity (3) at the same parameters W, ΔK, and ϑ_0 (curve *2*). The parameters are $W = 1$, $\Delta K = 1.2$, $d = 2$, and (a) $\vartheta_0 = 0.51$, (b) $\vartheta_0 = 0.6$, and (c) $\vartheta_0 = 0.78$.

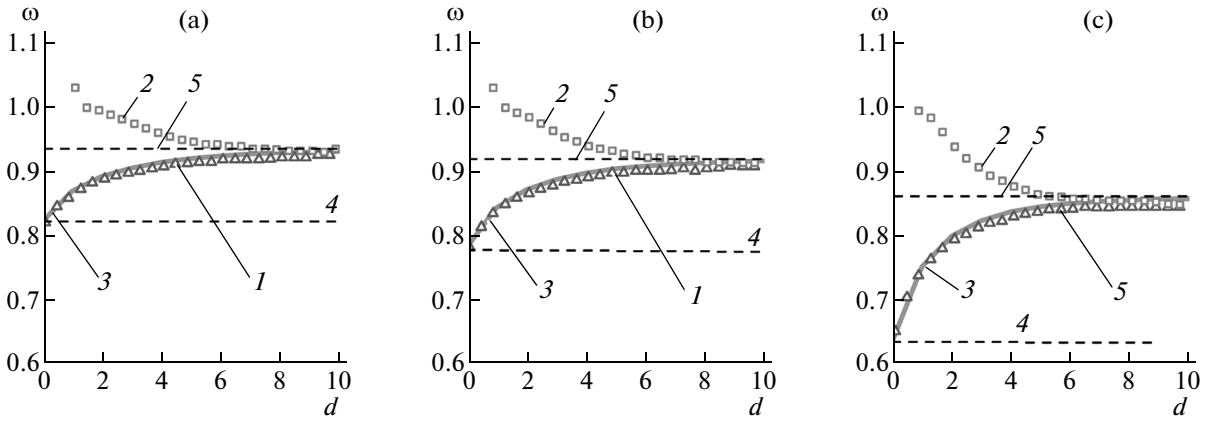

Fig. 8. dependence of Frequency characteristics of the impurity modes as functions of the distance d between the impurities for $W = 1$ and (a) $\Delta K = 0.8$, (b) $\Delta K = 0.9$, and (c) $\Delta K = 1.2$.

3. ANALYTICAL RESULTS

3.1. Model of Coupled Identical Oscillators

It was shown in [3, 17, 25] that a single impurity mode can be described analytically by applying the perturbation theory taking into account the excitation of a localized impurity mode in scattering a kink on a point impurity. In the case of two point impurities, it was shown in [43] that a system of second-order ordinary differential equations governing the oscillations of two identical harmonic oscillators with elastic coupling can be obtained [42, 44]:

$$\begin{aligned} \ddot{\varphi}_1 + \Omega_0^2 \varphi_1 &= F(\varphi_2 - \varphi_1), \\ \ddot{\varphi}_2 + \Omega_0^2 \varphi_2 &= -F(\varphi_2 - \varphi_1), \end{aligned} \tag{9}$$

where $\varphi_i = \varphi_i(t)$ is the deviation of the ith pendulum from equilibrium, $F = F(\Delta K, W, d)$ is a parameter characterizing the degree of coupling between the effective oscillators, and $\Omega_0 = \Omega_0(\Delta K, W, d)$ is the eigenfrequency of the effective oscillators.

To determine the dependences $\Omega_0(d)$ and $F(d)$ for three cases displayed in Fig. 8, we pass to the new coordinates

$$\xi_S = \frac{\varphi_1 + \varphi_2}{\sqrt{2}}, \quad \xi_A = \frac{\varphi_1 - \varphi_2}{\sqrt{2}}. \tag{10}$$

Then system (9) can be rewritten as follows (see [42]):

$$\begin{aligned} \ddot{\xi}_S + \Omega_0^2 \xi_S &= 0, \\ \ddot{\xi}_A + (\Omega_0^2 + 2F)\xi_A &= 0. \end{aligned} \tag{11}$$

Thus, the oscillations of the oscillators can be treated as the superposition of symmetric $\Omega_S = \Omega_0$ and antisymmetric $\Omega_A = (\Omega_0^2 + 2F)^{1/2}$ modes, which are known as the *normal modes* of the system, while variables (10) are called *normal coordinates.* In the special case of in-phase or antiphase oscillations, the system as a whole and each oscillator separately oscillate at the corresponding normal frequency. Thus, the frequency of the symmetric mode (Fig. 8, curve *1*) corresponds to the eigenfrequency of effective oscillators (9). To determine it, the indicated curves are approximated by a simple exponential [43]:

$$f(x) = A + B\exp(Cx),$$

where A, B, and C are approximation parameters. The approximation results are

$$\begin{aligned} \Omega_0(d) &= 0.92323 - 0.10130\exp(-0.48688d), \quad \Delta K = 0.8, \quad W = 1, \\ \Omega_0(d) &= 0.90603 - 0.12192\exp(-0.53047d), \quad \Delta K = 0.9, \quad W = 1, \\ \Omega_0(d) &= 0.84563 - 0.19752\exp(-0.65422d), \quad \Delta K = 1.2, \quad W = 1. \end{aligned}$$

Similarly, using the frequency of antisymmetric oscillations of the impurity modes (Fig. 8, curve *2*) and applying the relation $F = (\Omega_A^2 - \Omega_S^2)/2$, we can find

$$\begin{aligned} F(d) &= 0.00277 + 0.22733\exp(-0.40796d), \quad \Delta K = 0.8, \quad W = 1, \\ F(d) &= 0.00192 + 0.26571\exp(-0.43836d), \quad \Delta K = 0.9, \quad W = 1, \\ F(d) &= 0.00141 + 0.37745\exp(-0.53935d), \quad \Delta K = 1.2, \quad W = 1. \end{aligned}$$

Curves *1* and *2* in Fig. 8 depict the frequencies of in-phase and antiphase oscillations, respectively, obtained with the help of the Fourier analysis of the numerical solution to Eq. (1). Curve *3* was obtained by analytically solving Eq. (15). Curve *4* was obtained from (18); it shows the frequency of the breather in the case of a single impurity of double width for ω equal to (a) 0.8221, (b) 0.7825, and (c) 0.6382. Curve *5* was obtained from (16); it depicts the frequency of the breather in the case of a single impurity of the same size for ω equal to (a) 0.9342, (b) 0.9181, and (c) 0.8599.

Consider the case $d = 5$ and assume that the initial kinetic energy of the pendulums is zero: $\dot{\varphi}_i(0) = 0$; i.e., oscillations are excited only by an initial deviation. System (9) was numerically integrated from $t_{\min} = 0$ to $t_{\max} = 500$. Figure 9 presents three cases for which the initial conditions $\varphi_i(0)$ were the same as in Fig. 5.

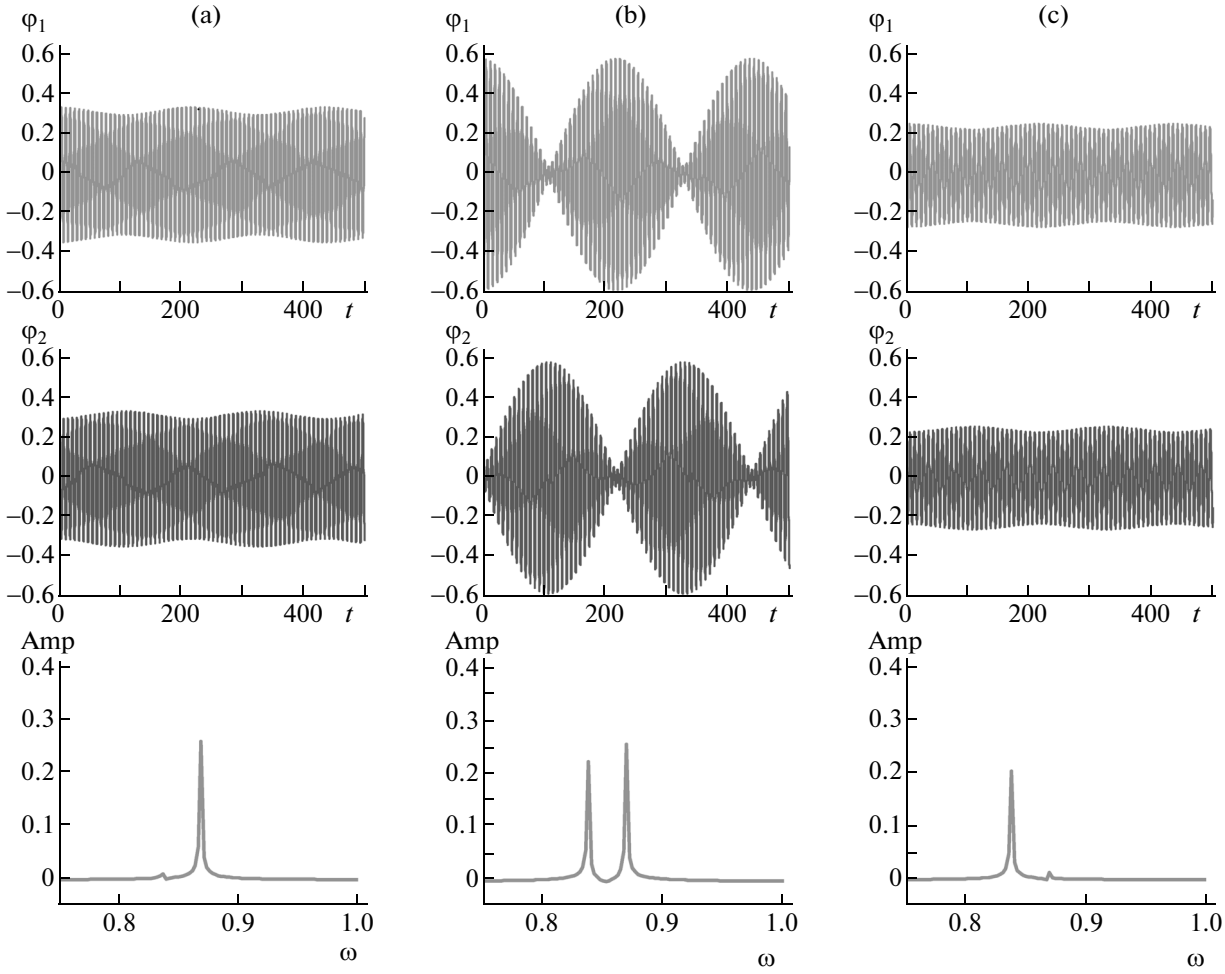

Fig. 9. Angles of deflection of the first φ_1 and second φ_2 oscillators in model (9) as functions of time t and the Fourier spectrum $\mathrm{Amp}(\omega)$ of $\varphi_1(t)$. The initial conditions are (a) $\varphi_1(0) = 0.338$, $\varphi_2(0) = -0.3$; (b) $\varphi_1(0) = 0.5821$, $\varphi_2(0) = -0.04$; and (c) $\varphi_1(0) = 0.2571$, $\varphi_2(0) = 0.23$.

We can see that the results are in good qualitative and quantitative agreement, which is also supported by the Fourier spectra.

Note also that, in the general case, the oscillations of the impurity modes are not harmonic, but their difference from harmonic behavior becomes important only for large oscillation amplitudes. In that case, for model (9), it is reasonable to consider other types of oscillators, for example, with sinusoidal nonlinearity. However, in the cases described in this paper (when impurity modes are excited by a kink scattered on an impurity and their amplitudes do not usually exceed 0.6), allowance for a sinusoidal nonlinearity does not lead to a noticeable difference, so the equations of harmonic oscillators work well.

3.2. Linearization of the Nonlinear Problem

It was shown in [38] that, in the case of a small single impurity, the linearization of the original problem yields the Schrödinger equation, which provides good qualitative and quantitative agreement with the numerical results.

Consider the location of the discrete impurity mode in the excitation spectrum of problem (1). Taking into account that the considered one-dimensional equation (1) with $K(x) = 1$ additionally has vacuum solutions, for example, $\theta_{\pm}(x, t) = 0$, we seek the spectrum of small excitations around them:

$$\psi(x, t) = \theta_{\pm}(x, t) + \delta\psi(x, t), \quad \delta\psi(x, t) = e^{-i\omega t}, \tag{12}$$

where $|\delta\psi(x, t)| \ll 1$. Substituting (12) into (1) and linearizing the equation with respect to $\delta\psi$, we obtain the Schrödinger equation

$$\frac{d^2}{dx^2}\psi + (\psi^2 - K(x))\psi = 0. \tag{13}$$

Consider a spatial modulation of the periodic potential $K(x)$ in the form of two identical rectangular potential wells (4). The domain is divided into five zones. A solution is sought in the form of exponential functions outside the impurities and in the form of trigonometric functions inside them:

$$\begin{aligned}
\psi_1(x) &= A_1 e^{-lx} + B_1 e^{lx},\\
\psi_2(x) &= A_2 \sin kx + B_2 \cos kx,\\
\psi_3(x) &= A_3 e^{-lx} + B_3 e^{lx},\\
\psi_4(x) &= A_4 \sin kx + B_4 \cos kx,\\
\psi_5(x) &= A_5 e^{-lx} + B_5 e^{lx}.
\end{aligned} \tag{14}$$

The characteristic equation has the form

$$k_0^2 + \omega^2 - 1 + \Delta K = 0, \quad k_0 = i\sqrt{\omega^2 + \Delta K - 1}, \quad k = \sqrt{\omega^2 + \Delta K - 1}.$$

Assume that $\omega^2 + \Delta K - 1 > 0$ and $1 - \omega^2 > 0$. A dispersion relation is derived by equating the functions and their derivatives with respect to the coordinate on the boundaries of the domains:

$$l^2 - k^2 + 2lk\cot kW = \pm(l^2 + k^2)e^{-ld}, \tag{15}$$

where $l = \sqrt{1 - \omega^2}$ and $k = \sqrt{\omega^2 + \Delta K - 1}$.

The validity of the result is verified by considering the limiting cases $d \longrightarrow 0$ and $d \longrightarrow \infty$. As $d \longrightarrow \infty$, the right-hand side of (15) tends to zero and the expression passes into a dispersion relation obtained previously in the case of a single impurity (see [38]):

$$l^2 - k^2 + 2lk\cot kW = 0. \tag{16}$$

For $d = 0$, we have

$$l^2 - k^2 + 2lk\cot kW = \pm(l^2 + k^2). \tag{17}$$

The plus and minus signs in (17) correspond to two classes of solutions: even and odd, respectively. Since, at $d = 0$, two impurities can be treated as a single effective one of width $2W$, we need to compare (17) with expression (16) for the case of a doubled-width impurity:

$$l^2 - k^2 + 2lk\cot(k \times 2W) = 0. \tag{18}$$

It can be shown that, in the limiting case of two merging impurities, the dispersion relation coincides with that for the case of a single impurity of double width.

Note that solution (14) covers several interesting special cases. For example, in-phase or antiphase oscillations of localized waves on impurities are possible. More specifically, in-phase oscillations are possible if $A_2 = A_4 = 0$ in (14), while antiphase oscillations are possible if $A_2 = B_4 = 0$. It is also possible that two interacting waves merge in a single one. Using (15), we construct the dependence $\omega(d)$ for three different cases (see Fig. 8, curve *3*). It can be seen that both limiting cases $d \longrightarrow 0$ and $d \longrightarrow \infty$ hold. Curve *5* in Fig. 8 depicts the frequency of the oscillation mode found analytically from (16) in the case of single impurity (3) with the same parameters ΔK and W; it represents the asymptote for curve *3*. Curve *4* was computed from (18) in a similar manner.

Figure 8 shows that dispersion relation (15) (curve *3*) is in good qualitative and quantitative agreement with the numerically computed symmetric mode (curve *1*). This is explained by the fact that expression (15) involves the eigenfrequency of the impurity modes, which coincides with the frequency of the symmetric mode (as follows from (11)).

4. CONCLUSIONS

The structure and the properties of four-kink multisolitons (called quadrons) in the form of localized coupled waves excited on impurities were studied. The cases of widely and closely spaced impurities were considered. The frequencies of nonlinear large-amplitude waves localized on the impurities were studied depending on the distance between the impurities. It was shown that the quadron oscillations are well described by the model of two coupled identical oscillators. Specifically, in a similar manner to the case of two coupled oscillators, two frequencies were observed in the oscillation spectrum. In the case of small-amplitude oscillations, the spectrum of their possible oscillation modes was studied analytically and good qualitative agreement with the numerical results was found.

REFERENCES

1. V. G. Bykov, *Nonlinear Wave Processes in Rock* (Dal'nauka, Vladivostok, 2000) [in Russian].
2. L. V. Yakushevich, *Nonlinear Physics of DNA* (Regulyarnaya i Khaoticheskaya Dinamika, Izhevsk, 2007).
3. O. M. Braun and Yu. S. Kivshar, *The Frenkel–Kontorova Model: Concepts, Methods, and Applications* (Springer, Berlin, 2004; Fizmatlit, Moscow, 2008).
4. M. A. Shamsutdinov, V. N. Nazarov, I. Yu. Lomakina, et al., *Ferro- and Antiferromagnetic Dynamics: Nonlinear Oscillations, Waves, and Solitons* (Nauka, Moscow, 2009) [in Russian].
5. G. L. Alfimov, "Nonlocal sine-Gordon equation: Kink solutions in the limit of weak nonlocality," Nelin. Din. **5**, 585–602 (2009).
6. R. N. Garifullin, L. A. Kalyakin, and M. A. Shamsutdinov, "Autoresonance excitation of a breather in weak ferromagnets," Comput. Math. Math. Phys. **47**, 1158–1170 (2007).
7. A. M. Kosevich and A. S. Kovalev, *Introduction to Nonlinear Physical Mechanics* (Naukova Dumka, Kiev, 1989) [in Russian].
8. N. R. Quintero, A. Sánchez, and F. G. Merten, "Existence of internal modes of sine-Gordon kinks," Phys. Rev. E **62** (1), R60–R63 (2000).
9. M. B. Fogel, S. E. Trullinger, A. R. Bishop, and J. A. Krumhansl, "Dynamics of sine-Gordon solitons in the presence of perturbations," Phys. Rev. B **15**, 1578–1592 (1977).
10. C. J. K. Knight, G. Derks, A. Doelman, and H. Susanto, "Stability of stationary fronts in a nonlinear wave equation with spatial inhomogeneity," J. Differ. Equations **254**, 408–468 (2013).
11. J. P. Currie, S. E. Trullinger, A. R. Bishop, and J. A. Krumhansl, "Numerical simulation of sine-Gordon soliton dynamics in the presence of perturbations," Phys. Rev. B **15**, 5567–5580 (1977).
12. V. G. Makhan'kov, "Solitons and numerical experiment," Sov. J. Part. Nucl. **14**, 50–75 (1983).
13. F. Zhang, Y. S. Kivshar, and L. Vazquez, "Resonant kink-impurity interactions in the sine-Gordon model," Phys. Rev. A **45**, 6019–6030 (1992).
14. B. Piette and W. J. Zakrzewski, "Scattering of sine-Gordon breathers on a potential well," Phys. Rev. E **79**, 046603 (2009).
15. M. B. Fogel, S. E. Trullinger, A. R. Bishop, and J. A. Krumhansl, "Classical particlelike behavior of sine-Gordon solitons in scattering potentials and applied fields," Phys. Rev. Lett. **36**, 1411–1414 (1976).
16. J. A. González, A. Bellorin, and L. E. Guerrero, "Internal modes of sine-Gordon solitons in the presence of spatiotemporal perturbations," Phys. Rev. E (Rapid Commun.) **65**, 065601 (2002).
17. Y. S. Kivshar, F. Zhang, and L. Vazquez, "Resonant soliton-impurity interactions," Phys. Rev. Lett. **67**, 1177–1180 (1991).
18. L. V. Yakushevich, G. R. Kashapova, and F. K. Zakir'yanov, "Influence of periodic field with constant and slowly changing frequency on movement of DNA kink," Biofizika **57** (1), 21–26 (2012).
19. D. I. Paul, "Soliton theory and the dynamics of a ferromagnetic domain wall," J. Phys. C: Solid State Phys. **12**, 585–593 (1979).
20. K. Javidan, "Analytical formulation for soliton-potential dynamics," Phys. Rev. E **78**, 046607 (2008).
21. T. I. Belova and A. E. Kudryavtsev, "Solitons and their interactions in classical field theory," Phys.-Usp. **40**, 359–386 (1997).
22. B. Piette and W. J. Zakrzewski, "Scattering of sine-Gordon kinks on potential wells," J. Phys. A: Math. Theor. **40**, 5995–6010 (2007).
23. E. G. Ekomasov, Sh. A. Azamatov, and R. R. Murtazin, "Studying the nucleation and evolution of magnetic inhomogeneities of the soliton and breather type in magnetic materials with local inhomogeneities of anisotropy," Phys. Metals Metallogr. **105**, 313–321 (2008).
24. V. A. Malomed and A. A. Nepomnyashchy, "Interaction of two fluxons near a local inhomogeneity in a long Josephson junction," Phys. Rev. B **45**, 12435–12441 (1992).
25. R. H. Goodman and R. Haberman, "Interaction of sine-Gordon kinks with defects: The two-bounce resonance," Physica D: Nonlin. Phenom. **195**, 303–323 (2004).

26. A. G. Bratsos, "The solution of the two-dimensional sine-Gordon equation using the method of lines," J. Comput. Appl. Math. **206** (1), 251–277 (2007).
27. Y. N. Gornostyrev, M. I. Katsnelson, A. Y. Stroev, and A. V. Trgfilov, "Impurity-kink interaction in the two-dimensional Frenkel–Kontorova model," Phys. Rev. B **71**, 094105 (2005).
28. E. G. Ekomasov, Sh. A. Azamatov, and R. R. Murtazin, "Excitation of nonlinear solitary flexural waves in a moving domain wall," Phys. Metals Metallogr. **108**, 532–537 (2009).
29. G. Kalberman, "The sine-Gordon wobble," J. Phys. A: Math. Gen. **37**, 11603–11612 (2004).
30. D. R. Gulevich and F. V. Kusmartsev, "Perturbation theory for localized solutions of the sine-Gordon equation: Decay of a breather and pinning by a microresistor," Phys. Rev. B **74**, 214303 (2006).
31. S. B. Kryuchkov and E. V. Kaplya, "Soliton delay line based on a semiconductor superlattice," Tech. Phys. **48**, 576–579 (2003).
32. J. A. González, S. Cuenda, and A. Sánchez, "Kink dynamics in spatially inhomogeneous media: The role of internal modes," Phys. Rev. E **75**, 036611 (2007).
33. E. G. Ekomasov, R. R. Murtazin, and A. M. Gumerov, "One-dimensional dynamics of domain walls in two-layer ferromagnet structure with different parameters of magnetic anisotropy and exchange," J. Magn. Magn. Mater. **339**, 133 (2013).
34. E. G. Ekomasov, R. R. Murtazin, and O. B. Bogomazova, "Dynamics of kinks of the modified sine-Gordon equation in the presence of a stepwise spatially modulated periodic potential," Nelin. Mir **11** (1), 51–57 (2013).
35. E. G. Ekomasov and M. A. Shabalin, "Simulation the nonlinear dynamics of domain walls in weak ferromagnets," Phys. Metals Metallogr. **101**, S48–S50 (2006).
36. G. Kälbermann, "A model for soliton trapping in a well," Chaos, Solitons Fractals **12**, 2381–2385 (2001).
37. E. G. Ekomasov, A. M. Gumerov, and I. I. Rakhmatullin, "Numerical simulation of pinning and nonlinear dynamics of domain walls in ferromagnets with defects," Vestn. Bashkir. Univ. **15**, 564–566 (2010).
38. E. G. Ekomasov, A. M. Gumerov, and R. R. Murtazin, "Excitement of solitons in the interaction of kinks of sine-Gordon equation with attracting impurity," Komp'yut. Issled. Model. **4**, 509–520 (2012).
39. A. M. Gumerov, E. G. Ekomasov, and R. R. Murtazin, "Simulation of domain wall dynamics in weak ferromagnets," Khroniki Ob"edinennogo Fonda Elektronnykh Resursov Nauka i Obrazovanie, No. 5 (2010).
40. J. K. Perring and T. H. R. Skyrme, "A model unified field equation," Nuclear Phys. **31**, 550–555 (1962).
41. A. M. Gumerov and E. G. Ekomasov, "Study of the effect of point defects on the nonlinear dynamics of magnetic nonuniformities," Pis'ma Material. **3** (2), 103–105 (2013).
42. M. I. Rabinovich and D. I. Trubetskov, *Oscillations and Waves in Linear and Nonlinear Systems* (Regulyarnaya i Khaoticheskaya Dinamika, Moscow, 2000; Kluwer Academic, Dordrecht, 2013).
43. E. G. Ekomasov, A. M. Gumerov, and R. R. Murtazin, "Nonlinear dynamics of the magnetic inhomogeneities in magnetic with modulation of the magnetic parameters," *International Conference on Nonlinear Equations and Complex Analysis* (Bannoe Lake, Russia, 2013), p. 24.
44. P. S. Landa, *Nonlinear Oscillations and Waves in Dynamical Systems* (Kluwer Academic, Dordrecht, 1996; Librokom, Moscow, 2010).

Translated by I. Ruzanova